

# Fibrillary Arrangement of Elongated, Almost Parallel Aggregates of Hydrophobic and Hydrophilic Domains Forming the Nafion Surface Structure Improved Contrast Atomic Force Microscopy Images

Omar Teschke,\* Juliana Andrea Franco Burguim, Wyllerson Evaristo Gomes, and David Mendez Soares



Cite This: *ACS Omega* 2023, 8, 49073–49079

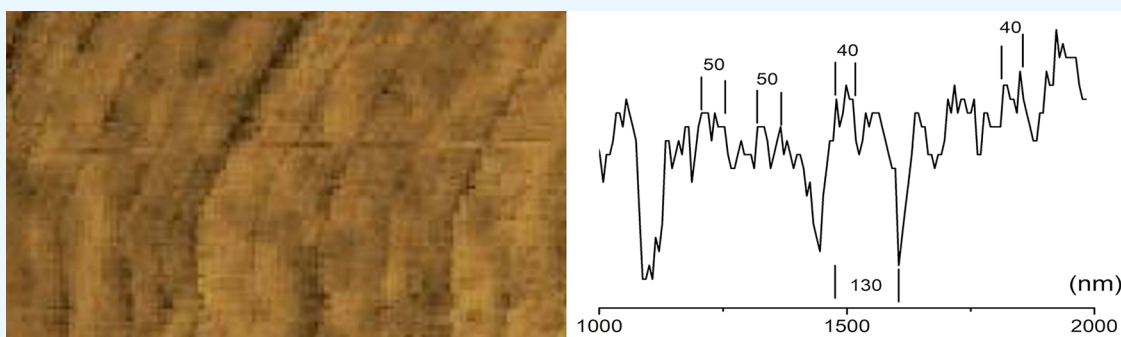


Read Online

ACCESS |

Metrics & More

Article Recommendations



**ABSTRACT:** A significant improvement in spatial resolution is reported in Nafion surface maps when compared to previous atomic force microscopy images of the Nafion surface scanned in air. The technique ability is to generate maps showing approximately few nanometer ( $\sim 2\text{--}5$  nm) patterns to the long fiber length ( $>2$   $\mu\text{m}$ ). Atomic force microscopy force vs separation curve profiles registered in water are used to characterize the surface hydrophobic and hydrophilic domains. Initially, Nafion surfaces were imaged in air for comparison and then immersed in water. Nafion surfaces immersed in water display a matrix of hydrophilic and hydrophobic regions with fibrillary structure dimensions of  $\sim 40$  nm formed by fiber pairs. Ribbons formed by two pairs with diameters of  $\sim 83$  nm are separated by larger channels.

## INTRODUCTION

Hydrogen-powered vehicles using polymer electrolyte membrane fuel cells have been demonstrated by auto manufacturers, and hydrogen-powered buses are in service in several cities. Nafion, operating as a separating membrane in pH differential electrolysis cells, was investigated in our previous studies.<sup>1,2</sup> Nafion is a poly(tetrafluoroethylene) (PTFE) polymer with hydrophilic perfluorovinyl pendant side chains terminated with sulfonic acid groups that acts as a common membrane separator owing to its chemical and thermal stabilities as well as high proton conductivity. The PTFE backbone ensures long-term chemical stability in reducing and oxidizing environments. The sulfonic headgroups on the side chains exhibit extremely high acidity due to electron-withdrawing  $-\text{CF}_2-$  groups.<sup>3</sup>

Nafion absorbs water that is separated into the domains of the hydrophilic and hydrophobic phases. Ion conductivity occurs through hydrophilic channels.<sup>4,5</sup> These hydrophilic channels of Nafion for proton conduction have inspired many studies over the past three decades since its discovery in the early 1970s. Previous studies centered on characterizing the structure and physical properties of Nafion membranes,

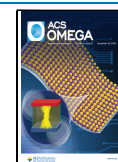
focusing on the structure of hydrophilic domains.<sup>6–8</sup> X-ray scattering studies yielded a model for the internal morphology of the membrane based on a hydrophilic region comprising clusters of ionic groups in a reverse micellar-type structure connected by small channels.<sup>6,7</sup> One of the first experiments to look directly at the water inside Nafion membranes was presented by Falk,<sup>9</sup> who used steady-state IR spectroscopy to study the properties of water in Nafion. The IR spectra demonstrated that water experiences a range of environments in Nafion and the hydrogen bond network in Nafion was weaker than that in bulk water.<sup>9,10</sup> Based on the IR spectra, Falk<sup>9</sup> proposed that the internal structure comprised a tortuous network of interconnected channels with considerable local heterogeneity. Further, small-angle neutron scattering studies and small-angle X-ray studies yielded a new model comprising

**Received:** September 11, 2023

**Revised:** November 27, 2023

**Accepted:** November 29, 2023

**Published:** December 11, 2023



fibrillary aggregates of hydrophobic polymer with hydrophilic side chains that protrude radially outward.<sup>4,11,12</sup> In this work, we are going to investigate the Nafion/water interfacial region by imaging the Nafion immersed in water and using force vs separation AFM profiles to determine hydrophobic and hydrophilic site distribution.

This work then describes an AFM scanning method that results in improved contrast images of curved Nafion surfaces encircling PTFE fibers, forming a mesh. It is then possible to determine the Nafion surface fibrillary structure dimensions.

## EXPERIMENTAL ANALYSES

Nafion N-222 and Nafion PTFE fabric reinforced with a polytetrafluoroethylene fiber are perfluorosulfonic acid cation

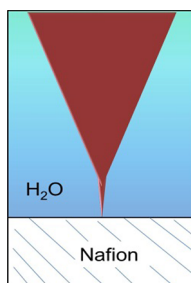


**Figure 1.** Schematic diagram of the tip/Nafion water interfacial region. The tip has a conical shape.

exchange membranes with thicknesses of 0.28 mm. Swollen membranes were prepared by increasing the temperature from 25 to 100 °C in a vessel for 8 h using pure water as the swelling agent. At least four pieces of reinforced PTFE and Nafion N-222 membranes were prepared. Pieces of the membrane were weighed in the dry state. After the swelling process, the swollen state of the membrane was determined; all of the samples showed typically a 20% increase in weight. Subsequently, the membrane was introduced in a measuring liquid cell, and force versus separation curves were registered. AFM force measurements were acquired by using a scanning probe microscope (model TMX2000, TopoMetrix, Veeco, Plainview, New York).

A sensor using a four-quadrant detector measures vertical and lateral forces. A special cell was built to perform observations in liquid media.<sup>13,14</sup> The cell was made of Teflon, and Nafion was fixed at its bottom. It was mounted in an *xyz*

piezotransmitter to position the sample in contact with a stationary tip. The laser beam enters and leaves the cell through a glass plate and thus does not cross the air–liquid interface, which is usually curved. Silicon nitride ( $\text{Si}_3\text{N}_4$ ) tips (Veeco, model MSCT-AUHW) with a spring constant of  $\sim 0.03$  N/m and a radius curvature of  $\sim 5$  nm were used. The instrument was calibrated, and the measured spring constant in air (0.03 nN/nm) was found to agree with that specified by the cantilever manufacturer.

The surface of a  $\text{Si}_3\text{N}_4$  tip in aqueous solution is composed of amphoteric silanol and basic silylamine (secondary and/or primary amines), although the latter is rapidly hydrolyzed) surface groups<sup>15,16</sup> at pH  $\sim 6$ . With no added electrolyte, the  $\text{Si}_3\text{N}_4$  surface is either zwitterionic (zero net charge) or slightly negatively charged;<sup>17</sup> consequently, we assumed that the surface charge density in the tip is null.

We explored the Nafion surface structure by measuring the force acting on the tip when it was immersed in water. For this purpose, atomic force microscopy (AFM) topographic views and force vs separation curves were used to characterize structurally different hydrophilic and hydrophobic regions.

The interfacial water-probing experiments were performed at room temperature (25 °C) in an environmental chamber housing the AFM. The results reported herein are based on several experiments using different Nafion samples and contact points within experiments. A schematic of the Nafion/water interface and probing tip is shown in Figure 1.

Background subtraction was used to determine the nanoscopic line profile, which is a filtering process used to eliminate sample background features for image analysis. The process applies an algorithm to the underside of the image surface. The algorithm subtracts out underlying features that are larger than or equal to the user-defined radius by eliminating the *Z* height data of the larger features, and the fine features on the sample surface are then resolved and can be used as a measurement technique for determining the lateral spacing in the line profile and peak spacing.

## RESULTS AND DISCUSSION

The interfacial region was probed using the force versus separation curves. The interfacial water is considered to be inhomogeneous because polarization (and permittivity) is a function of the distance to the surface.<sup>18</sup> The measured profiles are induced by the interfacially charged surface. Transition

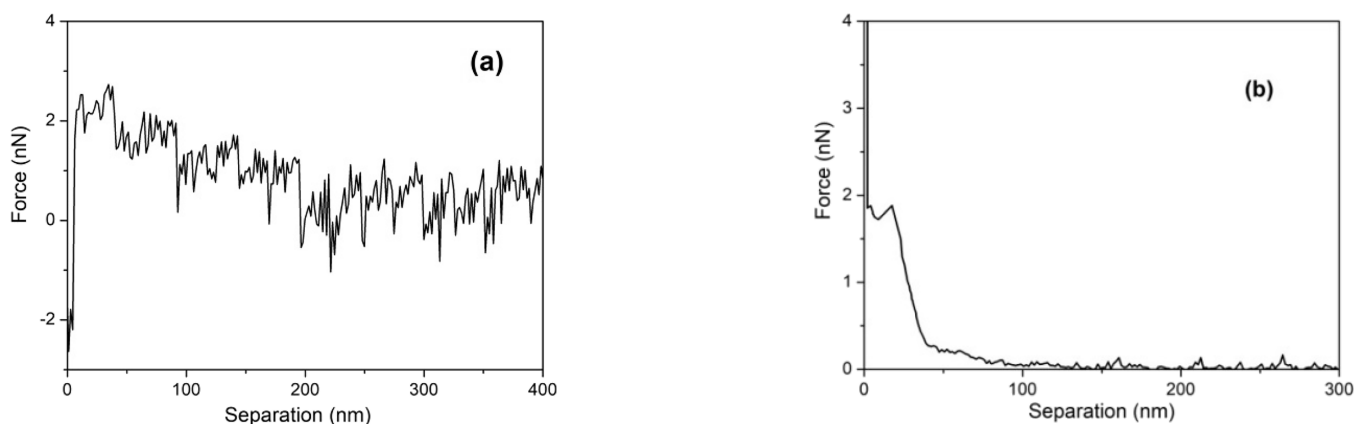


**Figure 2.** (a) Force vs separation curve measured when probing a region attached to a water/Nafion interface and (b) the same as in panel (a) when probing another region.

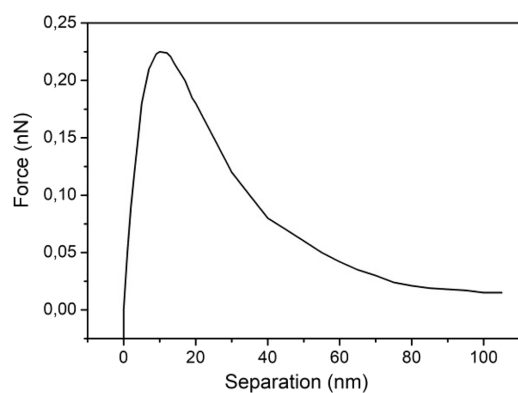


**Figure 3.** Force vs separation curve for a  $\text{Si}_3\text{N}_4$  tip and a mica sample immersed in water.

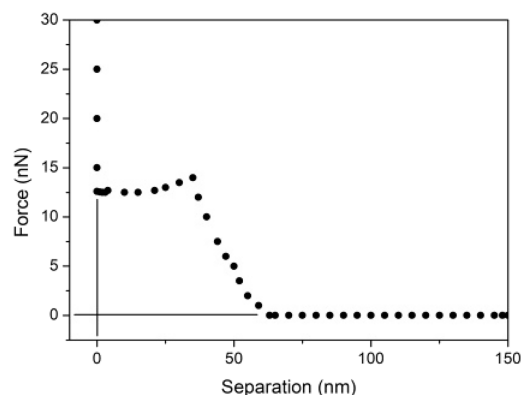


**Figure 4.** Force vs separation curve measured on a hydrophobic surface where repulsive forces are present at the regions close to the substrate ( $x = 0$ ).

zone profiles adjacent to the Nafion substrates immersed in water are explained below.

In these measurements, repulsive and attractive forces act on the tip before the sample contact. Hence, when the sample approaches the tip, the cantilever bends upward or downward. At a certain point, the tip is attracted to the surface. Finally, moving the sample still further causes a deflection of the cantilever by the same amount as that for which the sample is moved. The approaching force curve is a plot of the change in the cantilever deflection ( $\Delta Y$ ) versus sample displacement ( $\Delta X$ ). On a hard nondeformable surface,  $\Delta Y$  is proportional to  $\Delta X$  while the tip and sample are in contact. Rather than using

the sample position ( $X$ ), it is more useful to use an absolute distance ( $H$ ) that is relative to the separation between the tip and the sample surface. The correction to produce a force–separation curve uses the relationship  $H = \Delta X + \Delta Y$ .<sup>19</sup> The following force curves show the force versus separation absolute distance plots. AFM topographic views and force curve separation were used to characterize structurally different regions.

#### Force vs Separation Curves Associated with Hydrophobic and Hydrophilic Surfaces Immersed in Water.

**Figure 2a** depicts the force vs separation curve for a Nafion surface immersed in water. The presented profile can be interpreted as follows. Zero force is recorded beyond  $\sim 200$  nm because the AFM tip experiences negligible resistance moving through the bulk as it approaches the Nafion surface. This shows that AFM is insensitive to any structure that might exist in the bulk liquid. At  $\sim 200$  nm, an increasing force acts on the tip, and at  $\sim 10$  nm, the repulsive force is followed by an attractive force. **Figure 2b** shows the force vs separation curve obtained at a distinct region of the Nafion surface, showing only a repulsive profile in the interfacial region. Two distinct force vs separation curves are then registered when probing this surface.

To verify the Nafion hydrophobic/hydrophilic surface profile previously reported,<sup>4,11,12</sup> mica surfaces (hydrophilic substrate) and air/water interfaces (hydrophobic behavior) were probed and compared to the Nafion force vs separation profiles.

**Figure 3** shows the force versus separation curve measured on mica immersed in water. Mica is always negatively charged in water. When the mica basal plane is placed in water, the mechanism for the formation of the interfacial water region is assumed to be the dissolution of the  $\text{K}^+$  ions. It should be noted that the  $\text{K}^+$  ions initially held on the mica surface in the high resistivity water ( $18 \text{ M}\Omega/\text{cm}$ ;  $\sim 5 \times 10^{-6} \text{ M}$  1:1 electrolyte at  $\text{pH} \sim 6$ ) should be at least partially ion-exchanged.

The mica channel surface in water then shows hydrophilic force vs separation curves characterized by an attraction at the region close to the surface ( $\sim 10$  nm). The mica hydrophilicity was previously characterized.<sup>20–22</sup>

**Figure 4** shows the force versus separation curve measured on a hydrophobic surface. An air bubble ( $\sim 2 \text{ nm}$   $\varphi$ ) deposited on the PTFE substrate was used. On hydrophobic surfaces, there is a repulsive force component, while hydrophilic surfaces show attraction forces attached to the surface ( $\sim 0$ ). Patterns corresponding to the water interfacial region attached to

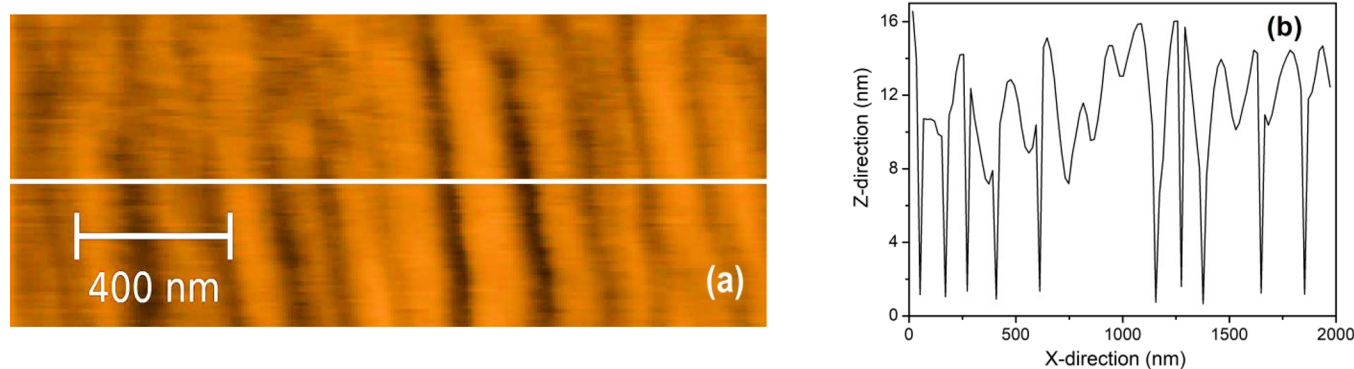


**Figure 5.** (a) Image of the AFM-scanned hydrated Nafion surface in air and (b) image profile of the white line in panel (a).

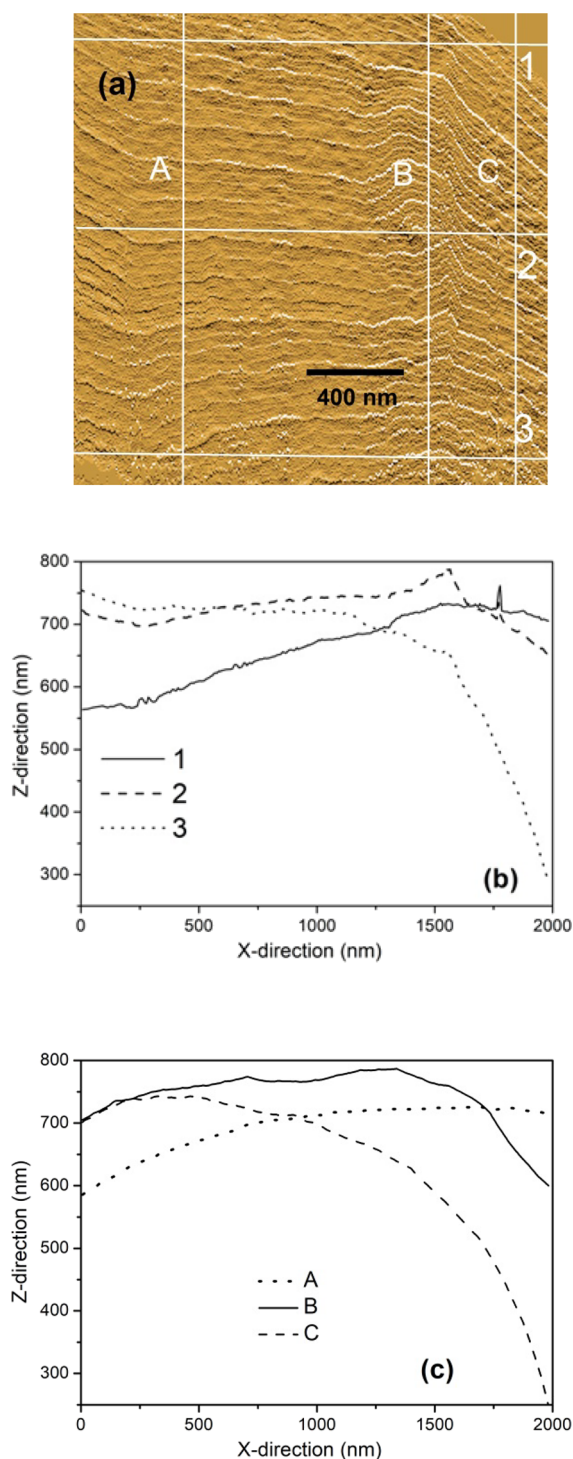


**Figure 6.** (a) AFM image displaying the pattern observed by scanning a Nafion surface immersed in water when a force of  $\sim 4$  nN is applied on the tip; (b) image profiles of the three white horizontal lines in panel (a) and (c) profile of three vertical lines in panel (a).

hydrophobic surfaces were previously published.<sup>23,24</sup> The pattern of the kink features of the force vs separation curve is reproducible, but their number/thicknesses/separation varies.<sup>24</sup>

Hydrophobic and hydrophilic region profiles were probed using force versus separation curves. Hydrophilic surfaces such as the mica surface immersed in water show the characteristic force vs separation profile depicted in Figure 3. A hydrophobic

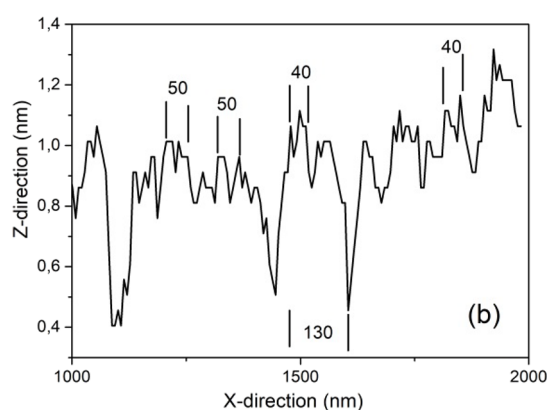
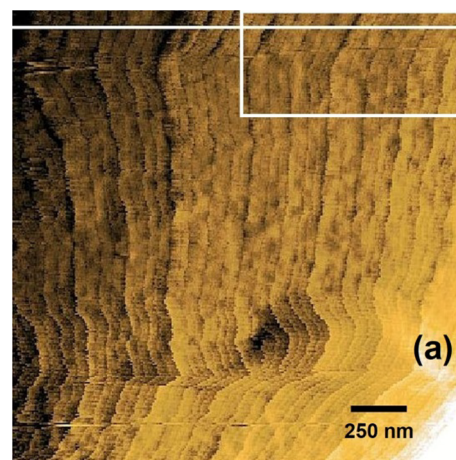


**Figure 7.** (a) AFM-scanned image (force of  $\sim 4$  nN is applied on the tip) of the hydrated Nafion surface in a region with an arrangement of parallel fibers showing individual fibers with  $\sim 20$  nm diameter and pairs with  $\sim 50$  nm and two pairs with  $\sim 130$  nm width. (b) White line image profile fibers separated by small channels forming pairs and pairs separated by channels forming ribbons plus large separation channels.

surface displays a different force vs separation profile as shown in Figure 4. By comparing Figure 2 with Figures 3 and 4, it is clear that the Nafion surface immersed in water presents regions with hydrophilic and hydrophobic responses when probed by AFM. Surface hydrophilic/hydrophobic section distribution will be characterized by AFM surface scanning.

**A Technique to Image Hydrophilic or/and Hydrophobic Sites Attached to Surfaces.** Specifically, we examine the surface site distribution of Nafion membranes using AFM mapping. The standard AFM contrast in images shows high structures as light regions and low structures as dark regions. For comparison, initially, we have an AFM-scanned hydrated Nafion surface in air. The results are shown in Figure 5a,b. Nafion surface morphology under hydrated conditions is described as a network of elongated yet segmented domains. An arrangement of parallel fibers with a separation of  $\sim 220$  nm is visible. The fiber diameters as observed by the light regions in the figure vary, an apparent height difference between the two layers (dark and light regions) of  $-10$  nm is measured and shown in Figure 5b, and fiber diameters as small as  $\sim 80$  nm are observed.

Figure 6a displays the pattern observed by scanning a Nafion surface immersed in water; as for images registered in air, high

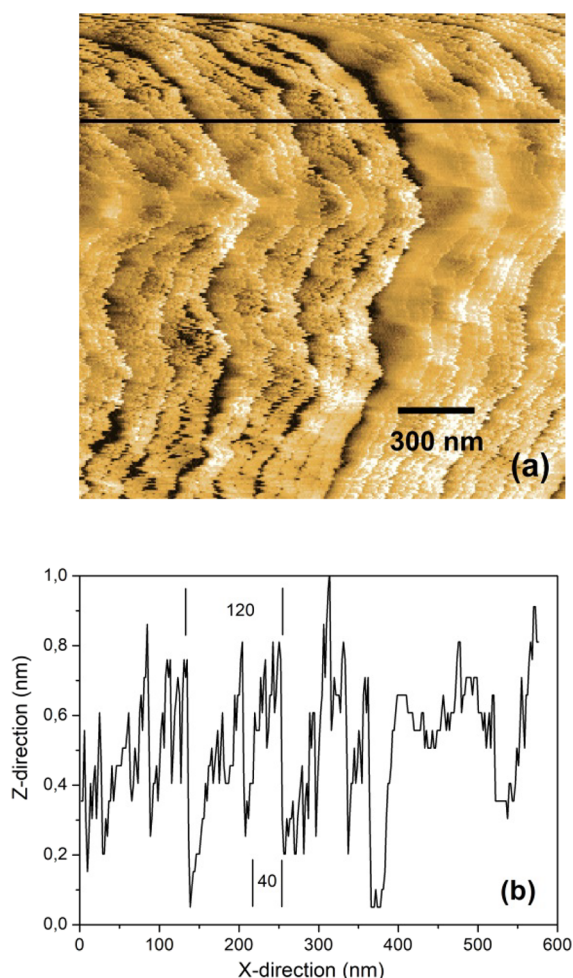


**Figure 8.** (a) AFM-scanned image (force of  $\sim 4$  nN is applied on the tip) of the hydrated Nafion surface in a region with a highly curved arrangement of fibers and (b) topographic image profile of the black line in panel (a). Pairs with 40 nm width and ribbons formed by two pairs plus separation distance result in an arrangement with 120 nm width.

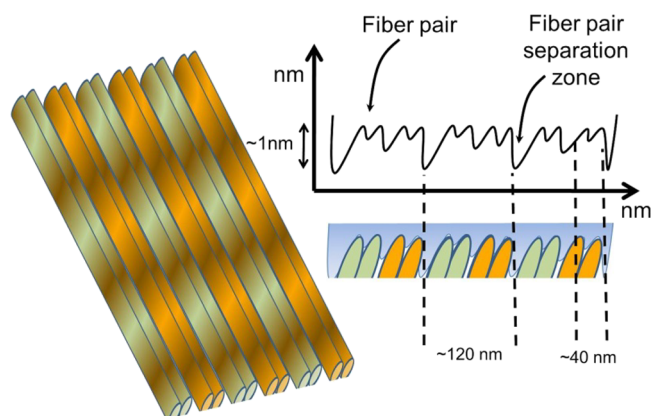


**Figure 9.** Schematic diagram of the Nafion surface-probed region showing a pair of fibers separated by channels forming  $\sim 83$  nm-diameter ribbons.

structures are shown as light regions. A pattern of fibers that are aligned horizontally with various curved regions is observed. Profiles at three distinct horizontal lines indicated by 1, 2, and 3 are shown in Figure 6b, and the surface is not flat

but shows a variable curved profile. Figure 6c shows the profile of the vertical line indicated by A, B, and C.

Considerable forces between the tip and the sample are required for AFM imaging. For hard samples, such as mineral surfaces, these forces do not generally lead to any sample penetration. However, for soft films, the minimum forces are barely enough to allow stable imaging. To obtain the conventional AFM contrast in the scanned samples, an analysis of the force versus distance curves is a requirement as follows: let us observe Figure 2 and consider the following simple scenario where we have an almost null vertical component due to the tip gliding. At the light region (hydrophilic portion in Figure 2a), by setting the contact force at  $\sim 4$  nN, the tip is not contacting the top of the soft layer. When the tip reaches the dark region (hydrophobic portion in Figure 2b), the repulsive force is smaller than that at the light region, and consequently, the tip gets in contact with the substrate.

Figure 7 shows an arrangement of parallel fibers observed on the Nafion surface immersed in water. The image profile indicated by the white line in Figure 7a is depicted in Figure 7b. To determine its fine structure profile, a background subtraction was applied.

Finally, Figure 8a shows a region with a highly curved arrangement of fibers. Dark regions correspond to lower structures. The background subtraction procedure was also applied, and the corresponding profile of nanosized spikes is shown in Figure 8b. This region depicts an arrangement of fibers showing a pair with  $\sim 40$  nm width and ribbons with  $\sim 120$  nm width. The same dimensions are observed in the sample shown in Figure 7.

#### Almost Parallel Fibers Separated by Nanochannels.

Hydrophilic and hydrophobic site distribution as observed by AFM imaging of Nafion membranes immersed in water is going to be described next. Force vs separation curves and AFM images were used to probe the nanoscale surface domain distributions and their dimensions. Hydrophilic sulfonic acid side group phases are known to separate from Nafion hydrophobic fluorocarbon backshores previously determined using small-angle X-ray studies.<sup>4,11,12</sup> Arrangements of these surface domains are shown in Figures 7 and 8 where hydrophobic sites are indicated by dark regions and hydrophilic regions by light regions.

Since it is difficult to extract a more accurate size of the fibril cross section using images registered in water, we have made a background subtraction, a procedure described in *Experimental Analyses*. After background subtraction, topographic profiles as shown in Figures 7b and 8b are registered. The Nafion surface response looks like modulated at the submicrometer scale. In Figure 7a, two fibers forming pairs and two pairs forming ribbons are shown. The two pairs are separated from the other pairs in contact by deep channels. The four fibers forming two pairs with a width of  $\sim 120$ – $130$  nm are separated by channels indicated in a black color.

In some other locations,  $\sim 100$ – $160$  nm-wide cylindrical structures are observed. The diameter of each fiber forming the two pairs is  $\sim 20$  nm, with a separation of  $\sim 20$  nm. The black region separating the two pairs has a width of  $\sim 20$ – $40$  nm. A schematic diagram of this arrangement is shown in Figure 9. This pattern shows an almost regular arrangement with the thickness of the fibers and their separation. The width of the deep and shallow channels may be measured using the profiles shown in Figures 7b and 8b. A pattern featuring polymer ribbons separated by channels is visible as well as a wide

channel separating two fiber pairs and thin channels separating individual fibers.

AFM images of the surface morphology reveal dramatic differences when compared with images obtained under ambient conditions (air).

Figure 5 shows images of fibers scanned in air with a diameter as small as  $\sim 80$  nm; fiber diameter dimensions of Nafion immersed in water are shown in Figure 7b. Ribbons of two pairs have a diameter of  $\sim 80$  to 120 nm. It is then possible to observe that these  $\sim 80$  nm-diameter profiles are imaged by both techniques. The different profiles were associated with the dielectric exchange force<sup>25</sup> responsible for the force acting on the tip when scanning hydrophilic and hydrophobic surfaces and present only on tips immersed in water.

These results are also in agreement with the previous results claiming that hydrophilic channels attached to hydrated Nafion substrates protrude<sup>4,11,12</sup> radially outward. Another study<sup>5</sup> has shown that the hydrated Nafion surface is formed by an arrangement of hydrated sulfonic acid groups surrounded by a hydrophobic substrate, forming fibrillary features.

The total length of the aggregate fibers is not visible in our images, but there is a tendency to form a network of almost parallel fibers. Figure 7b shows that it is possible to resolve the individual aggregate packed into ribbons of two pairs. So, the profile permits to extract the ribbon dimensions, distinct hydrophobicity, and fibrillary morphology.

## CONCLUSIONS

The aim of the paper is to determine the spatial organization of the fibrillary aggregates forming the Nafion surface, first at small scales within few nanometer resolution (separation channel width) and second at a large scale in the submicrometer range. By AFM probing of hydrated Nafion surfaces immersed in water, it is possible to observe that there are two distinct force vs separation profiles (see Figures 2–4) shown as regions with attractive and repulsive profiles measured on the Nafion membrane surface. We have then shown that the Nafion membrane surface structure is characterized by a nanophase separation between hydrophilic and hydrophobic domains,<sup>26–28</sup> previously described but not imaged, with a ribbon-like polymeric aggregate arrangement.

The size of hydrophilic domains is around  $20 \pm 5$  nm, which form pairs, and two pairs join to form ribbons. The observed structure has 2 distinct channel profiles separating fiber pairs and fibers. Then, an important feature of the wormlike superstructures is that they consist of two fibers forming ribbons that give the cylindrical character of the surface aggregates. These features comprise segments of elongated, wormlike patterns that tortuously extend along the membrane surface, forming almost parallel arrangements. Such elongated features stretch up at least to  $\sim 40 \mu\text{m}$  in length, confirming predictions of large features made by Kim et al.<sup>29</sup> based on ultrasmall-angle neutron scattering.

## AUTHOR INFORMATION

### Corresponding Author

Omar Teschke – Laboratório de Nanoestruturas e Interfaces, Instituto de Física, UNICAMP, Campinas, SP 13083-859, Brazil; [orcid.org/0000-0002-1152-9319](https://orcid.org/0000-0002-1152-9319); Email: [oteschke@ifi.unicamp.br](mailto:oteschke@ifi.unicamp.br)

## Authors

Juliana Andrea Franco Burguim – Laboratório de Nanoestruturas e Interfaces, Instituto de Física, UNICAMP, Campinas, SP 13083-859, Brazil

Wyllerson Evaristo Gomes – Faculdade de Química, Pontifícia Universidade Católica de Campinas, Campinas, SP 13012-970, Brazil

David Mendez Soares – Laboratório de Nanoestruturas e Interfaces, Instituto de Física, UNICAMP, Campinas, SP 13083-859, Brazil

Complete contact information is available at:

<https://pubs.acs.org/10.1021/acsomega.3c06927>

## Notes

The authors declare no competing financial interest.

## ACKNOWLEDGMENTS

The authors are grateful to J. R. Castro for technical assistance.

## REFERENCES

- (1) Teschke, O.; Zwanziger, M. G. Operation of a Steady State pH-Differential Water Electrolysis Cell. *Int. J. Hydrogen Energy* **1982**, *7*, 933–937.
- (2) Teschke, O. Theory and Operation of a Steady State pH Differential Water Electrolysis Cell. *J. Appl. Electrochem.* **1982**, *12*, 219–223.
- (3) Blake, N. P.; Petersen, M. K.; Voth, G. A.; Metiu, H. Structure of Hydrated Na-Nafion Polymer Membranes. *J. Phys. Chem. B* **2005**, *109*, 24244–24253.
- (4) Gebel, G. Structural evolution of water swollen perfluorosulfonated ionomers from dry membrane to solution. *Polymer* **2000**, *41*, 5829–5838.
- (5) Moilanen, D. E.; Piletic, I. R.; Fayer, M. D. Water Dynamics in Nafion Fuel Cell Membranes: The Effects of Confinement and Structural Changes on the Hydrogen Bond Network. *J. Phys. Chem. C* **2007**, *111*, 8884–8891.
- (6) Gierke, T. D.; Munn, G. E.; Wilson, F. C. The morphology in Nafion perfluorinated membrane products, as determined by wide- and small-angle x-ray studies. *J. Polym. Sci.: Polym. Phys.* **1981**, *19*, 1687–1691.
- (7) Hsu, W. Y.; Gierke, T. D. Elastic theory for ionic clustering in perfluorinated ionomers. *Macromolecules* **1982**, *15*, 101–105.
- (8) Yeo, S. C.; Eisenberg, A. Physical properties and supermolecular structure of perfluorinated ion-containing (Nafion) polymers. *J. Appl. Polym. Sci.* **1977**, *21*, 875–898.
- (9) Falk, M. An infrared study of water in perfluorosulfonate (Nafion) membranes. *Can. J. Chem.* **1980**, *58*, 1495–1499.
- (10) Moilanen, D. E.; Piletic, I. R.; Fayer, M. D. Tracking waters response to structural changes in Nafion membranes. *J. Phys. Chem. A* **2006**, *110*, 9084–9088.
- (11) Rubatat, L.; Gebel, G.; Diat, O. Fibrillar structure of Nafion: Matching Fourier and real space studies of corresponding films and solutions. *Macromolecules* **2004**, *37*, 7772–7778.
- (12) Rubatat, L.; Rollet, A. L.; Gebel, G.; Diat, O. Evidence of elongated polymeric aggregates in Nafion. *Macromolecules* **2002**, *35*, 4050–4056.
- (13) Teschke, O.; Douglas, R. A.; Prolla, T. A. Viscous drag effect on imaging of linearized plasmid deoxyribonucleic acid in liquid medium with the atomic force microscope. *Appl. Phys. Lett.* **1997**, *70*, 1977–1979.
- (14) Sasaki, R. M.; Douglas, R. A.; Kleinke, M. U.; Teschke, O. Structure imaging by atomic force microscopy and transmission electron microscopy of different light emitting species of porous silicon. *J. Vac. Sci. Technol. B* **1996**, *14*, 2432–2437.
- (15) Bergstrom, L.; Bostedt, E. Surface chemistry of silicon nitride powders: Electrokinetic behaviour and ESCA studies. *Colloids Surf., A* **1990**, *49*, 183–197.

- (16) Harane, D. L.; Bousse, L. J.; Shott, J. D.; Meindl, J. D. Ion-sensing devices with silicon nitride and borosilicate glass insulators. *IEEE Trans. Electron Devices* **1987**, *34*, 1700–1707.
- (17) Teschke, O.; Ceotto, G.; de Souza, E. F. Imaging of soft structures: Dependence of contrast in atomic force microscopy images on the force applied by the tip. *J. Vac. Sci. Technol. B* **2000**, *18*, 1144–1150.
- (18) Hunter, R. J. *Foundations of colloid science*, Oxford University Press, 2001, p 806.
- (19) Butt, H. J.; Jaschke, M.; Ducker, W. Measuring surface forces in aqueous electrolyte solution with the atomic force microscope. *Bioelectrochem. Bioenerg.* **1995**, *38*, 191–201.
- (20) Teschke, O.; Ceotto, G.; de Souza, E. F. Dielectric Exchange Force: a Convenient Technique for Measuring the Interfacial Water Dielectric Permittivity Profile. *Phys. Chem. Chem. Phys.* **2001**, *3*, 3761–3768.
- (21) Teschke, O.; Ceotto, G.; de Souza, E. F. Interfacial Water Dielectric-Permittivity-Profile Measurement Using Atomic Force Microscopy. *Phys. Rev. E* **2001**, *64*, 11605–11610.
- (22) de Souza, E. F.; Ceotto, G.; Teschke, O. Dielectric Constant Measurements of Interfacial Aqueous Solutions Using Atomic Force Microscopy. *J. Mol. Catal. A: Chem.* **2001**, *167*, 235–243.
- (23) Teschke, O.; de Souza, E. F. Water Molecule Cluster Measured at Water/Air Interfaces using Atomic Force Microscopy. *Phys. Chem. Chem. Phys.* **2005**, *7*, 3856–3865.
- (24) Teschke, O.; de Souza, E. F. Hydrophobic Surfaces Probed by Atomic Force Microscopy. *Langmuir* **2003**, *19*, 5357–5360.
- (25) Teschke, O.; de Souza, E. F. Electrostatic response of hydrophobic surface measured by atomic force microscopy. *Appl. Phys. Lett.* **2003**, *82*, 1123–1126.
- (26) Fujimura, M.; Hashimoto, T.; Kawai, H. Small-angle x-ray scattering study of perfluorinated ionomer membranes. 2. Models for ionic scattering maximum. *Macromolecules* **1982**, *15*, 136–144.
- (27) Roche, E. J.; Pineri, M.; Duplessix, R.; Levelut, A. M. Small-Angle Scattering Studies of Nafion Membranes. *J. Polym. Sci., Polym. Phys.* **1981**, *19*, 1–11.
- (28) Gierke, T. D.; Hsu, W. Y. The Cluster-Network Model of Ion Clustering in Perfluorosulfonated Membranes. *ACS Symp. Ser.* **1982**, *13*, 283–307.
- (29) Kim, M.-H.; Glinka, C. J.; Grot, S. A.; Grot, W. G. SANS Study of the Effects of Water Vapor Sorption on the Nanoscale Structure of Perfluorinated Sulfonic Acid (Nafion) Membranes. *Macromolecules* **2006**, *39*, 4775–4787.